Theoretical Study of the MoS_2 (100) Surface: A Chemical Potential Analysis of Sulfur and Hydrogen Coverage

S. Cristol, J. F. Paul, and E. Payen*

Laboratoire de Catalyse de Lille, CNRS/UPRESA 8010, Bât. C3, Université des Sciences et Technologies de Lille F-59655 Villeneuve d'Ascq Cedex, France

D. Bougeard

Laboratoire de Spectrochimie Infrarouge et Raman, CNRS/UPR 2631 Bât. C5, Université des Sciences et Technologies de Lille F-59655 Villeneuve d'Ascq Cedex, France

S. Clémendot and F. Hutschka

Total Raffinage Distribution, CERT, BP 27, F-76700 Harfleur, France

Received: July 3, 2000; In Final Form: September 12, 2000

The stability of the (100) MoS_2 surface has been studied using periodic DFT calculations taking into account various parameters such as the temperature and the partial pressure ratios of H_2 and H_2S present in the surrounding atmosphere. It appears that the sulfur coverage of the surface is strongly dependent on the H_2/H_2S ratio and that under working conditions, the most stable surface does not contain any coordinately unsaturated sites (CUS). Direct comparisons with experimental literature data such as EXAFS or TPR measurements show a good agreement between calculations and these experiments. The second part of the study deals with the behavior of hydrogen on the surfaces. The endothermic dissociation always leads to Mo−H and S−H groups. This implies that hydrogen is not stable on the MoS_2 surface unless at very high pressure or very low temperature. Furthermore, H_2 dissociation on the surface will not lead to the formation of CUS.

1. Introduction

Hydrodesulfurization (HDS) is the most important catalytic process used to remove sulfur from petroleum fractions. The increasing demand to convert sulfur-rich feedstocks and the environmental pressure for further reductions in the sulfur content of oil products lead to a need for more efficient processes and more active catalysts. The type of catalyst most used for HDS is Co(Ni)Mo/Al_2O_3, which consists of well-dispersed molybdenum disulfide nanocrystallites supported on γ-alumina and promoted by cobalt or nickel atoms. MoS_2 has a layered structure and it has been shown that these MoS_2 nanocrystallites are more or less stacked, the mean number of slabs being between one and four.[1] It is generally assumed that under the experimental conditions with a H_2/H_2S mixture, sulfur vacancies are created at the edge of the MoS_2 slabs; these vacancies are considered as active sites.[2] In spite of the numerous works dedicated to these solids, no experimental data are available for the precise description of the nature of these sites, i.e., the sulfur and/or hydrogen coverage of these edge surfaces under reaction conditions. Modeling of these nanocrystallites is one possible approach to get a better insight into the nature of the sites as well as in the HDS mechanism. A relatively low number of works were devoted to the modelization of the nonpromoted active phases. Harris and Chiannelli[3] used SCF-Xα method for such purposes but the size of their clusters was too small to be considered as representative of the active phase. Mitchell et al. presented density functional theory (DFT) calculations of small Mo−S clusters,[4] and in previous studies we presented DFT calculations of a $Mo_{12}S_{24}$ cluster.[5] These studies showed that it was necessary to take into account a large number of atoms to avoid computational artifacts. Periodic calculations should thus be an interesting alternative to describe these molybdenum disulfide active phases. Byskov et al.[6] used such a method for a MoS_2 linear chain. Raybaud et al.[7] published an ab initio investigation of the structural and electronic properties of the clean MoS_2 (100) edge surface using the Vienna ab initio simulation program (VASP). These authors showed that the cleaved edge surface remains stable in vacuum up to temperatures of $T = 700$ K. More recently, these authors demonstrated that the stoichiometry of the crystallite varies with the chemical potential of sulfur and thus could analyze the relative stability of various surfaces with respect to the gaseous environment.[8]

The aim of the present paper is to derive a similar approach putting an emphasis on the gaseous phase in order to determine the stability of the MoS_2 edge surfaces under a broad range of experimental working conditions of the catalyst (*P*, *T*, and partial pressures). In the following sections the computational methods and the quantum mechanical models with various S/Mo ratio will be presented. Then their stability versus the relative partial pressure of H_2 and H_2S will be discussed. As the presence of hydrogen on this active phase is also a matter of debate, H_2 dissociation on these surfaces and the hydrogen coverage will also be considered in the second part of this study. A direct correlation with experimental literature data will be carried for the two types of surface.

2. Computational Methods

For our calculations, we used the Vienna Ab Initio Simulation Program (VASP).[9] It is based on Mermin's finite-temperature local density functional theory.[10] The calculations are performed

10.1021/jp0023819 CCC: $19.00
Published on Web 11/04/2000

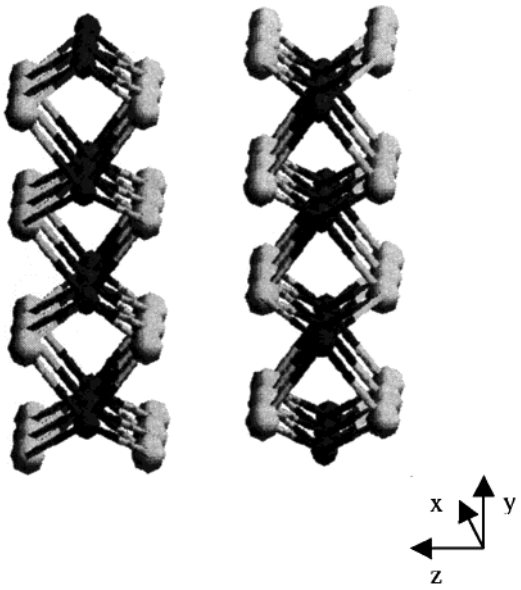

Figure 1. Perfect MoS_2 (100) surface [6−0]: light circles, sulfur atoms; dark circles, molybdenum atoms. The structure is periodic along the *x* and *z* directions.

in a plane wave basis set and the electron−ion interactions are described using optimized ultrasoft pseudopotentials.[11] The resolution of the Kohn−Sham equations is performed using an efficient matrix diagonalization routine based on a sequential band by band residual minimization method for the one electron energies. An improved Pulay mixing is used to update the charge density. The optimization of the atomic positions is performed via a conjugate gradient minimization of the total energy using the Hellmann−Feyman forces on the atoms. We refer to ref 9 for a more detailed description of the technique.

Throughout this work, we used a large supercell ($9.48 \times 20 \times 12.294$ Å^3) containing three unit cells in the *x* direction, four in the *y* direction, and two layers along *z* axis. Raybaud et al.[7] showed that this model was suitable to predict the electronic and structural properties of the MoS_2 perfect surface. The two upper rows were allowed to relax while the two lower were kept fixed at the bulk geometry in order to simulate bulk constraints. The calculations were performed at Γ point with a cutoff energy of 210 eV, a Methfessel−Paxton[12] smearing with $\sigma = 0.1$ eV and the exchange-correlation functional developed by Ceperley and Alder and parametrized by Perdew and Zunger.[13] Generalized gradient corrections were introduced as proposed by Perdew et al.[14]

3. Sulfur Coverage

3.1. Thermodynamic Aspect. The perfect (100) MoS_2 surface is presented in Figure 1. It shows two layers, one exposing unsaturated molybdenum atoms ($10\bar{1}0$ edge), the other one exhibiting sulfur saturated Mo atoms ($\bar{1}010$ edge) that we name, hereafter, molybdenum and sulfur edge, respectively. In industrial working conditions that involve the presence of H_2 and H_2S in the gas/liquid phase, the edges of these active phases should be modified. Indeed, H_2S can depose sulfur on the unsaturated molybdenum atoms whereas H_2 can react with sulfur atoms present on the surface to create vacancies and produce H_2S. The energy of S addition and S removal can be calculated according to reaction 1.

$$\text{surface } 1 \pm n\text{H}_2 \leftrightarrow \text{surface } 2 \pm n\text{H}_2\text{S} \qquad (1)$$

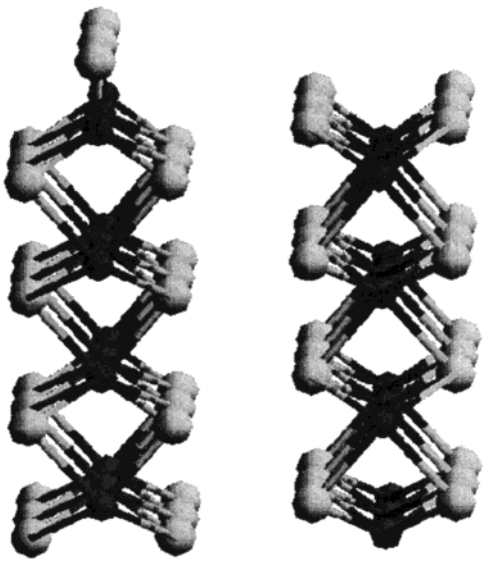

Figure 2. Cell showing the MoS_2 surface [6−3] (reference); stable surface when $-4.86 < \Delta\mu < -4.18$ eV i.e., $0.05 < H_2S/H_2 < 10\,000$ (see text).

TABLE 1: Electronic Contribution to $\Delta_r G$ for Reaction 2

surface	*n*	ΔE_{el} (eV)	surface	*n*	ΔE_{el} (eV)
6−6	−3	0.49	6−0	3	5.93
6−5	−2	0.90	5−3	1	0.77
6−4	−1	0.54	4−3	2	1.15
6−3	0	0.00	3−3	3	1.56
6−2	1	1.29	2−3	4	3.52
6−1	2	3.45	1−3	5	6.55

The various surfaces will be referred hereafter according to the number of sulfur atoms present on each edge of the surface of our model. We will note [6−0], a surface with six sulfur atoms on the sulfur edge and no sulfur atom on the molybdenum one. The calculated electronic energies of each surface are reported in Table 1 and show that the most stable surface according to equilibrium (1) is surface [6−3] with three adsorbed sulfur on the molybdenum edge (Figure 2). Instead of using the ideal crystallographic surface as a reference, we prefer to use the electronically most stable surface to analyze the influence of the gas phase. We now have to compute the Gibbs free energy of creation of the vacancies according to reaction 2. The surface [*x*−*y*] will be more stable than surface [6−3] as soon as $\Delta_r G$, which take into account the gas-phase nature, is negative.

$$\text{surface } [6-3] + n\text{H}_2 \leftrightarrow \text{surface } [x-y] + n\text{H}_2\text{S} \qquad (2)$$

$$\Delta_r G = \mu(\text{surface}[x-y]) - \mu(\text{surface}[6-3]) + n(\mu(\text{H}_2\text{S}) - \mu(\text{H}_2))$$

Throughout this work, we will assume that for condensed phases, the differences between the chemical potentials can be approximated by the difference between their computed electronic energies. This approximation which has been widely used,[15] gives good results as the temperature and pressure dependent terms of each condensed phase are close and tend to cancel in the free energy differences calculation. We can thus write

$$\Delta_r G = \Delta E^\circ + n\Delta\mu$$

where ΔE° is the difference between the electronic energy of the considered surfaces and $\Delta\mu$ is the difference between hydrogen sulfide and hydrogen chemical potentials. This equa-

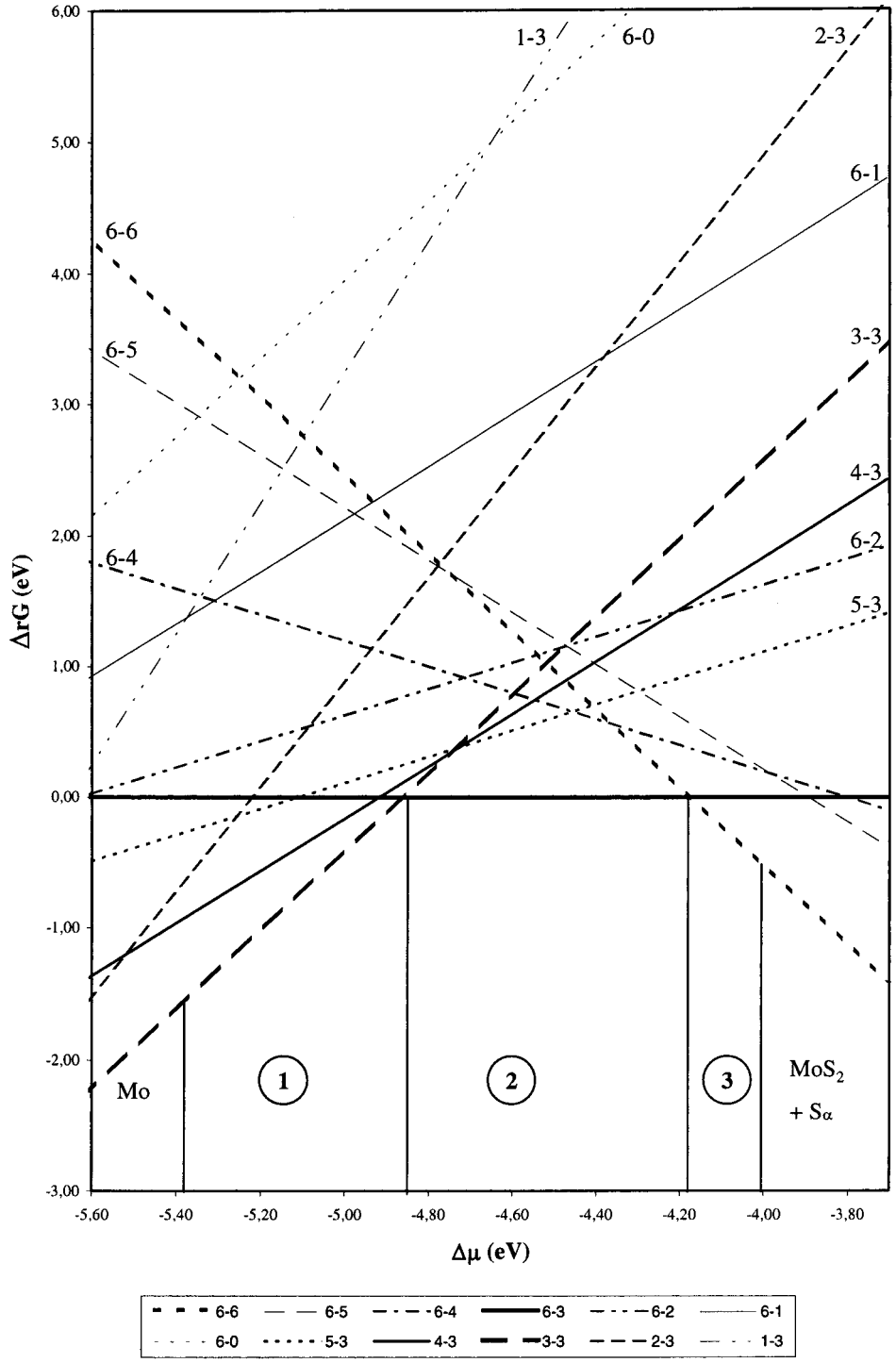

Figure 3. Variation of the Gibbs free energy of the sulfur coverage versus the chemical potential of the gas phase and the stability domain of the various surface stoichiometry.

tion leads to a linear dependence between $\Delta_r G$ and $\Delta\mu$, which will appear for each surface in Figure 3. $\Delta E°$ is computed with VASP for each stoichiometry and the temperature and pressure dependent terms $\Delta\mu$ can be obtained by the following equation:

$$\Delta\mu = \mu(H_2S) - \mu(H_2) = \Delta\mu°(T) + RT \ln \frac{P(H_2S)}{P(H_2)}$$

For each component of the gas phase, we have to add the thermal contributions to the computed electronic energy in order to obtain $\Delta\mu°(T)$.

$$\Delta\mu°(T) = \Delta E_{el} + \Delta ZPE + \Delta H_{vib} + \Delta H_{rot} + \Delta H_{tr} - T(\Delta S_{vib} + \Delta S_{tr} + \Delta S_{rot})$$

These contributions can be computed with the partition functions of each molecule using the standard formulas of statistical thermodynamics.[16] The calculations were performed at $T = 350$ °C, which approximately corresponds to the working temperature of the catalyst. It is now possible to calculate $\Delta_r G$ for various H_2S/H_2 partial pressure ratios from which the stoichiometry of the surface for each experimental condition can be deduced. Table 2 gives some $\Delta\mu$ numerical values obtained for various H_2S/H_2 molar ratio in the gas phase that

TABLE 2: $\Delta\mu$ Evaluation as a Function of the H_2S/H_2 Ratio at $T = 350$ °C

H_2S/H_2	$\Delta\mu$ (eV)	H_2S/H_2	$\Delta\mu$ (eV)
10000	−4.21	0.1	−4.83
1000	−4.34	0.01	−4.96
100	−4.46	0.001	−5.08
10	−4.59	0.0001	−5.21
1	−4.71		

are in the MoS_2 stability domain as computed below. For practical applications, the variation range of $\Delta\mu$ must be defined according to the concurrent chemical reactions of this complex system. Obviously, the reduction of MoS_2 on one side and of sulfur on the other side will fix the experimental range of $\Delta\mu$.

The reduction of the molybdenum disulfide into metallic molybdenum according to reaction 3 can be considered as the limit for increasing the hydrogen chemical potential.

$$MoS_2 + 2H_2 \leftrightarrow Mo + 2H_2S \quad (3)$$

This limit can be evaluated by the calculation of the Gibbs free energy of reaction 3 according to the following equation:

$$\Delta_r G = \mu(Mo) - \mu(MoS_2) + 2\Delta\mu = E°(Mo) - E°(MoS_2) + 2\Delta\mu$$

$E°(Mo)$ and $E°(MoS_2)$ were evaluated with VASP using the crystallographic structures. It appears that reduction should occur if $\Delta\mu$ is lower than −5.4 eV ($H_2S/H_2 < 10^{-6}$). MoS_2 is therefore not stable for a H_2S/H_2 ratio lower than 10^{-6}, conditions that would induce the formation of metallic molybdenum.

On the other side, for the high values of the sulfur chemical potential, the limit of the H_2S/H_2 ratio will be given by eq 4. Indeed it is not possible to reach a higher H_2S chemical potential as formation of sulfur will occur that will impose the H_2S/H_2 ratio.

$$H_2S \leftrightarrow S_\alpha + H_2 \quad (4)$$

Similarly the numerical value of this limit has been deduced from the calculation of the Gibbs free energy of reaction 4.

$$\Delta_r G = \mu(S_\alpha) - \Delta\mu = E°(S_\alpha) - \Delta\mu$$

$E°(S_\alpha)$ is computed with VASP from its crystallographic structure with 128 atoms per unit cell. It appears that the reaction becomes possible if $\Delta\mu$ is greater than −4.0 eV ($H_2S/H_2 > 10^6$). Indeed sulfur deposition occurs if sulfidation is performed without H_2 in the sulfiding mixture.[17]

However, those values have to be taken for their numerical range order. Indeed, in the HDS conditions, MoS_2 reduction may not lead to bulk metallic molybdenum and the reduction limit should be affected by the divided nature of the molybdenum disulfide. Similarly, sulfur can also occur in different allotropic varieties. Furthermore, the assumption ($E = \mu$) that we used is a rough approximation for reactions 3 and 4 as we deal with absolute chemical potential and not with chemical potential differences as in reaction 2. For example, the ZPE contributions of the solids will almost cancel in reaction 2 although they will not for reaction 3 and 4.

Figure 3 shows the $\Delta_r G$ variations for each surface as a function of $\Delta\mu$ taking surface [6−3] as reference. It can be seen that within the range of chemical potential we are studying, there are only three stability domains. Zone 1 of the diagram ($\Delta\mu < -4.86$ eV) is the high hydrogen chemical potential region corresponding to a $H_2S/H_2 < 0.05$. In this zone, the stable surface is surface [3−3], the scheme of which is represented on Figure 4. In the zone 2, the intermediate range of $\Delta\mu$ ($-4.86 < \Delta\mu < -4.18$ eV), the stable surface is surface [6−3]. The third zone of the diagram corresponds to high sulfur chemical potential and is obtained only when the H_2S/H_2 ratio is greater than 10 000. In this region, the surface is the totally saturated surface [6−6] represented on Figure 5. It should be noted that although a different approach is used in ref 9, these authors find the same stable surface in the range of sulfur chemical potential they studied (i.e., $H_2S/H_2 = 0.1$ to 0.01). However, taking reaction 2 as a reference allows a more direct correlation between calculations and experimental conditions.

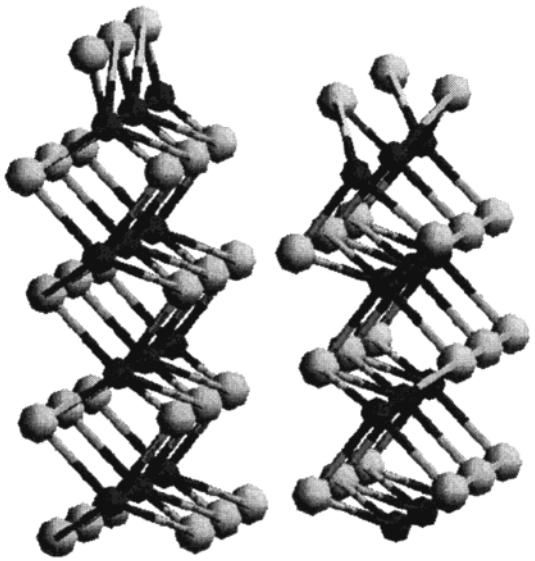

Figure 4. Cell showing the MoS_2 surface [3−3]; stable surface when $\Delta\mu < -4.86$ eV i.e., $H_2S/H_2 < 0.05$.

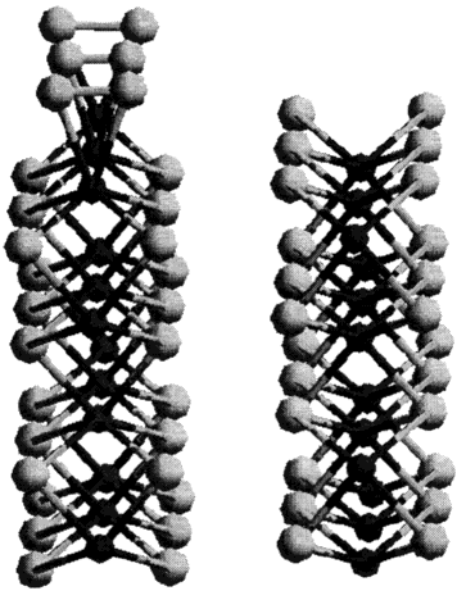

Figure 5. Cell showing the MoS_2 surface [6−6]; stable surface when $\Delta\mu > -4.18$ eV i.e., $H_2S/H_2 > 10\ 000$.

3.2. Comparisons with Experimental Data. As we can compute the stoichiometry of the MoS_2 surface for different experimental conditions, in order to check the validity of our calculations and to explain some experimental results we compare our results with some available experimental data. For this comparison we have to transpose our infinite periodic model to finite size crystallites. We will use the hexagonal geometrical

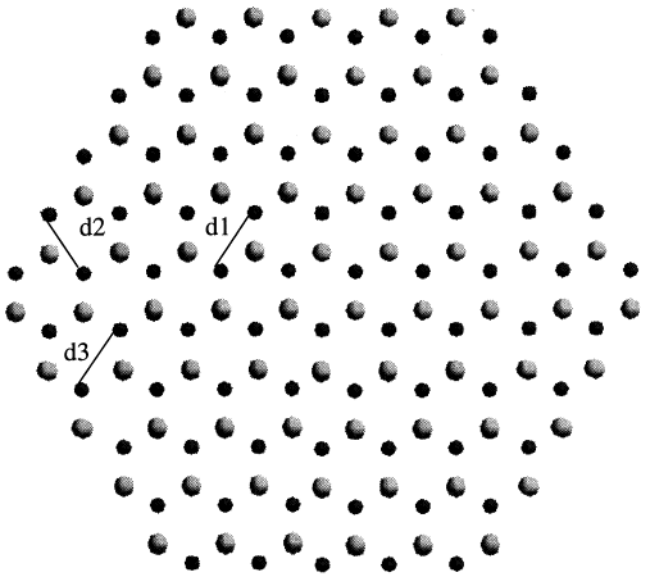

Figure 6. Hexagonal MoS_2 crystallite. d1, d2, and d3 are the distances defined by Shido and Prins (see ref 20).

TABLE 3: Mo-Mo Distances As Defined by Shido and Prins (Ref 20 and Figure 6) and in Our Different Models

	d1 (Å)	d2 (Å)	d3 (Å)
EXAFS	3.16	3.32	3.32
surface 6−6	3.16	3.10	3.22
surface 6−3	3.16	3.22	3.22
surface 3−3	3.16	3.22	3.06
surface 6−0	3.16	3.12	3.22

model developed by Kasztelan et al.[18] assuming that we can extend the results obtained on each edge of the calculated surface to the corresponding edge of the crystallite.

For the structural analysis, we will use EXAFS data obtained by Calais et al.[19] and revised by Shido and Prins.[20] To obtain reliable particle size, the latter authors showed that it was necessary to consider distortions on the edges on the MoS_2 crystallites. These distortions were characterized, as shown in Figure 6, by the distances d2 and d3 between neighboring molybdenum atoms situated at the two types of edges whereas d1 designated the Mo−Mo distance characteristic of the bulk structure. By fitting the particle size obtained with their method to TEM measurements, they deduced the distances that are reported in Table 3. It can be seen that the edge Mo−Mo distances are both longer than the bulk one. On the same table the computed bond distances obtained for the various stable surfaces described in section 3.1 are reported as well as the 6−0 surface ones. It appears that only the surface [6−3] presents an increase of the Mo−Mo distances on both edges. The other surfaces do not present similar surface relaxations. This is in agreement with the experimental EXAFS data that were obtained on a sample after sulfidation. Indeed, in these conditions (H_2S/H_2 = 15/85), the computed stable surface is surface [6−3]. However, the distortions obtained by Shido and Prins are more important than the ones we found. The reason for this difference might be that these authors considered a "perfect" MoS_2 crystallite and never took into account the sulfur coverage that would affect the average coordination number of the edge molybdenum atoms and therefore modify the EXAFS simulations.[21]

The sulfur coverage can be evaluated from a combined use of transmission electron microscopy (TEM) and temperature-programmed reduction (TPR) experiments published by Da Silva.[22] Their TPR experiments were performed on catalysts sulfided in a H_2S/H_2 (10/90) mixture that were cooled to room temperature in an H_2S/N_2 (10/90) mixture. After correction of H_2S desorption from alumina, the amount of H_2S produced between 100 and 290 °C is assigned to the sulfur atoms that were on the edges of the crystallites. The determination of the average particle size by TEM allowed these authors to determine the number of Mo atoms present on the edge of the disulfide crystallites. Finally, they deduced that one H_2S molecule is produced per edge molybdenum atom. From our theoretical calculations it can be considered that, at the beginning of the TPR (no H_2), the stable surface is the surface [6−6] that will evolute to the [3−3] surface during the TPR. Our calculations corroborate nicely the TPR experiments as going from surface [6−6] to surface [3−3], one H_2S molecule is eliminated per surface molybdenum atom.

It clearly appears that it is possible to compute the stoichiometry of the edge surfaces taking into account the atmosphere in which the catalyst is. The main point of the present study is that under the hydrodesulfurization working conditions ($T \sim$ 350 °C, $H_2S/H_2 < 0.01$), the stable surface is the [3−3] surface which does not present any CUS allowing adsorption of large molecules such as dibenzothiophene (DBT) or 4,6-dimethyldibenzothiophene (4,6DMDBT), these molecules being known as the most refractory compounds to the HDS process.[23] Active sites have thus to be created from surface [3−3] and can be obtained on both edges of the MoS_2 (100) surface. The energy required to create these CUS can be computed taking into account the temperature and pressure dependent terms. Calculation performed with T = 350 °C and H_2S/H_2 = 0.01 showed that it is easier to create a vacancy on the molybdenum edge (0.67 eV) than on the sulfur edge (1.34 eV). Whichever edge we consider, site creation appears as the thermodynamic limiting step of the HDS process for benzothiophene and larger molecules.[24] Decoration of the MoS_2 nanocrystallites with Co or Ni atoms may modify this step in decreasing the energy of creation of these CUS. This could explain the promoting effect of cobalt or nickel as discussed by Byskov et al.[6] in the bond energy model or by Toulhoat et al.[25] with the Sabatier principle. Indeed, cobalt and nickel have weaker metal to sulfur binding energy than molybdenum sulfur one. Raybaud et al.[26] confirmed this hypothesis in a following study showing that the sulfur coverage of the crystallite edges is also strongly dependent on the amount of promoter present on the surface. For a given sulfur chemical potential, the sulfur coverage decreases when the amount of promoter increases allowing the stable surfaces to present vacancies.

4. Hydrogen Coverage

4.1. Thermodynamical Aspect. The presence of hydrogen on the surface of the active crystallites is a matter of debate. Its presence is always required in HDS mechanistic studies,[27] however, if the existence of S−H groups have been suggested, direct evidences of Mo−H groups by physical characterization methods have never been reported. We have, therefore, investigated the hydrogen coverage of the disulfide nanocrystallites. We will write the hydrogenation of the edge surface as follows:

$$\text{bare surface } (S_0) + n\ H_2 \leftrightarrow \text{hydrogenated surface}(S_n) \quad (5)$$

The variation of the Gibbs free energy associated with reaction 5 can be written as

$$\Delta_r G = \Delta_r G^\circ - nRT \ln P(H_2)/P^\circ$$

$$\Delta_r G^\circ = \mu^\circ(S_n) - \mu^\circ(S_0) - n\mu^\circ(H_2)$$

The Gibbs free energy $\Delta_r G°$ can be calculated with the partition function of hydrogen gas and adsorbed hydrogen as written below:

$$\Delta_r G°(T) = \Delta U(0\ \mathrm{K}) - RT \ln \frac{q(S_n)}{q(S_0)q(H_2)^n}$$

Upon adsorption on the surface, the rotational and translational degrees of freedom of the H_2 molecule are changed into vibrational modes. As only a small numbers of atoms are added to the solid, we assumed that the changes in the vibrational density of state are negligible (i.e., $q(S_n) \sim q(S_0)$). The chemical potential difference between the two surfaces is therefore well approximated by the electronic energy variation. Thus $\Delta_r G$ can be written as

$$\Delta_r G°(T) = \Delta E_{el} + n\Delta \mathrm{ZPE} + nRT \ln(q(H_2))$$

with

$$\Delta E_{el} = E_{el}(S_n) - E_{el}(S_0) - nE_{el}(H_2)$$

$$n\Delta \mathrm{ZPE} = \mathrm{ZPE}(S_n) - \mathrm{ZPE}(S_0) - n\mathrm{ZPE}(H_2)$$

To evaluate this last term, we consider that the contributions of the adsorbed hydrogen and of the surface can be evaluated separately. We therefore write

$$n\Delta \mathrm{ZPE} = \mathrm{ZPE}(S_0) + n\mathrm{ZPE}(H_{2surf}) - \mathrm{ZPE}(S_0) - n\mathrm{ZPE}(H_2)$$

$$\Delta \mathrm{ZPE} = \mathrm{ZPE}(H_2\mathrm{surf}) - \mathrm{ZPE}(H_2)$$

Finally

$$\Delta_r G = \Delta E_{el} + n\alpha(T,P)$$

with

$$\alpha(T,P) = \Delta \mathrm{ZPE} + RT \ln (q(H_2)) - RT \ln \frac{P(H_2)}{P°}$$

$\alpha(T,P)$ that contains the temperature- and pressure-dependent contributions to the free energy variation appears as the variable parameter in this equation.

4.2. Hydrogenated Surfaces. A stability diagram of each hydrogenated surface as a function of the $\alpha(T,P)$ parameter can thus be drawn. As we are interested in the presence of hydrogen in the working conditions of the catalyst, the hydrogen coverage will be investigated for $H_2S/H_2 = 1/100$. In these conditions, section 3 showed that the stable surface is surface [3−3] with three remaining sulfur atoms on the sulfur edge and three adsorbed sulfur atoms on the molybdenum edge. For each edge, all the possible configurations from no hydrogen present on the surface to one H_2 molecule per surface molybdenum atom will thus be computed as follows: the dissociation of one H_2 molecule producing two S−H groups, two Mo−H groups or one S−H and one Mo−H will be first considered. The most stable configuration will be determined, on which we will consider similarly the dissociation of a second H_2 molecule. Finally, the dissociation of a third hydrogen molecule is considered on the most stable hydrogenated surface. In our calculations we will consider that both edges are in equilibrium with the gas phase; but these equilibriums are independent of each other. Thus sulfur exchange between these edges can only occur through the gas phase.

TABLE 4: H_2 Dissociation Electronic Energies According to Reaction 5 on the Molybdenum Edge of the MoS_2 Crystallites

	E(dissociation) (eV)
surface [*X*−3]	0.00
surface [*X*−3] Mo−H S−H	0.27
surface [*X*−3] 2 S−H	0.37
surface [*X*−3] 2 Mo−H 2 S−H	0.62
surface [*X*−3] 3 Mo−H 3 S−H	0.86
surface [*X*−2] 2Mo−H 2 S−H	1.39[a]

[a] Values including the vacancy creation energy at $T = 350$ °C and $H_2S/H_2 = 0.01$ (0.67 eV).

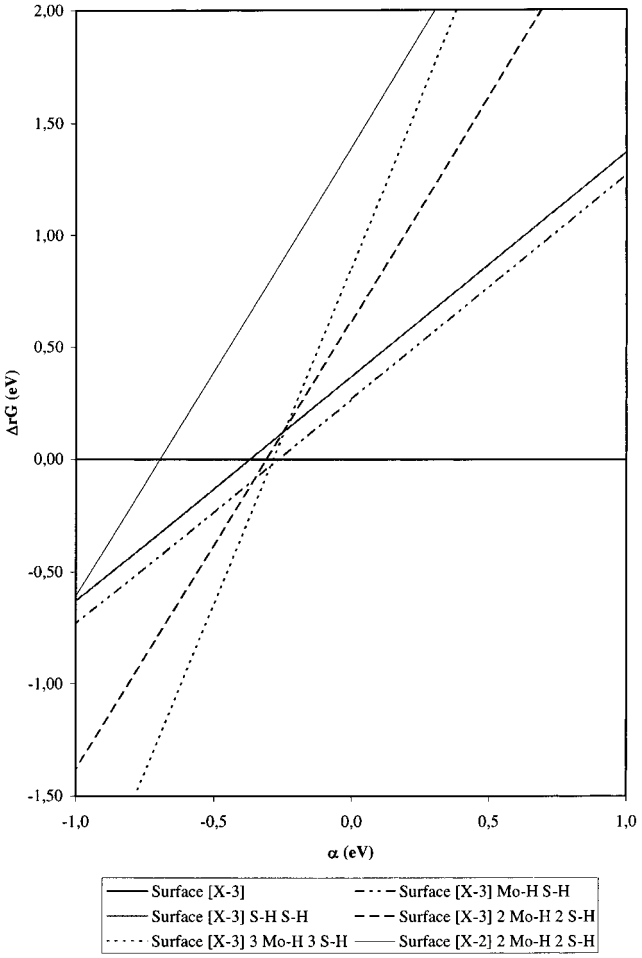

Figure 7. Variation of the Gibbs free energy of the reaction of H_2 dissociation on the molybdenum edge of the MoS_2 slab as a function of $\alpha(T,P)$.

(a) Molybdenum Edge [*X*−3]. On the molybdenum edge, H_2 dissociation is always endothermic according to the electronic energies reported in Table 4. The less endothermic process is the dissociation of the molecule into one S−H and one Mo−H group. Formation of two S−H groups requires more energy whereas the formation of two Mo−H groups appears impossible as one of the hydrogen atoms shifts from the molybdenum to the sulfur atom during the geometry optimization. The same tendencies are observed for the second and third hydrogenation. Figure 7 shows the variation of the Gibbs free energy of the successive hydrogenation associated to reaction 5, drawn as a function $\alpha(T,P)$. It can be deduced that for α values higher than −0.29 eV, i.e., at low hydrogen chemical potential, no hydrogen is present on the stable surface. Hydrogen is present on the surface only in the region corresponding to a $\alpha(T,P)$ value below

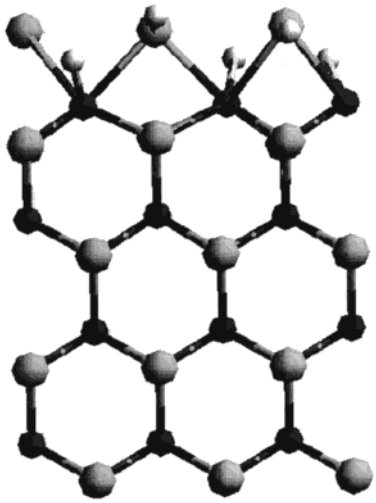

Figure 8. Cell showing the trihydrogenated MoS_2 molybdenum edge; stable for $\alpha(T,P) < -0.29$ eV.

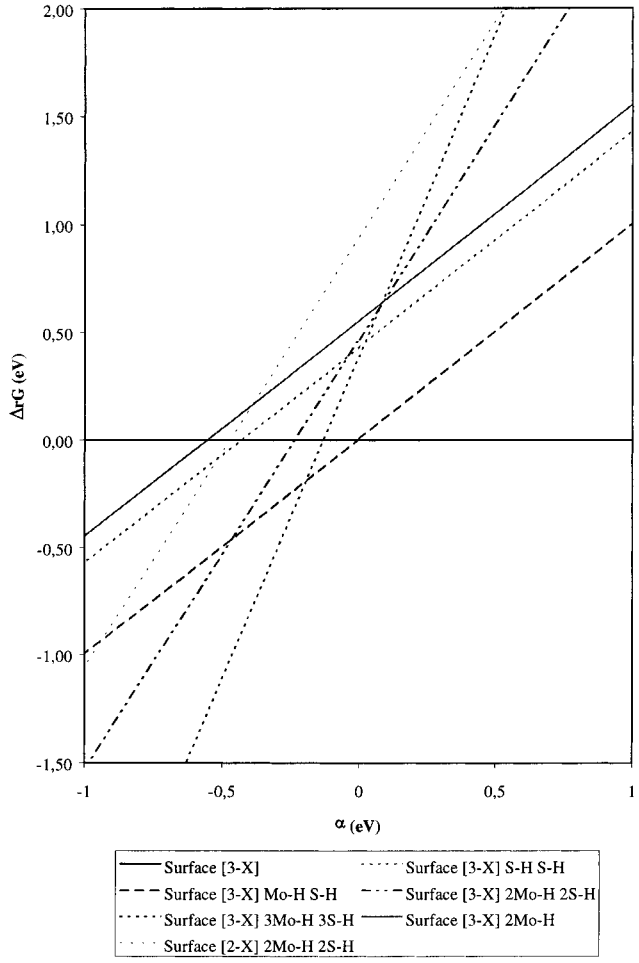

Figure 9. Variation of the Gibbs free energy of the reaction of H_2 dissociation on the sulfur edge of the MoS_2 slab as a function of $\alpha(T,P)$.

-0.29 eV that correspond to high hydrogen chemical potential as shown hereafter. In this region the surface is totally covered with hydrogen as S−H and Mo−H groups: each surface molybdenum atom and each surface sulfur atom is bound with hydrogen giving the surface which is schematically represented in Figure 8.

TABLE 5: H_2 Dissociation Electronic Energies According to Reaction 5 on the Sulfur Edge of the MoS_2 Crystallites

	E(dissociation) (eV)
surface [3−*X*]	0.00
surface [3−*X*] Mo−H S−H	0.01
surface [3−*X*] 2S−H	0.43
surface [3−*X*] 2Mo−H	0.56
surface [3−*X*] 2Mo−H 2S−H	0.47
surface [3−*X*] 3Mo−H 3S−H	0.39
surface [2−*X*] 2Mo−H	0.93[a]
surface [2−*X*] Mo−H S−H	1.44[a]
surface [2−*X*] 2Mo−H 2S−H	0.95[a]

[a] Values including the vacancy creation energy at $T = 350$ °C and $H_2S/H_2 = 0.01$ (1.34 eV).

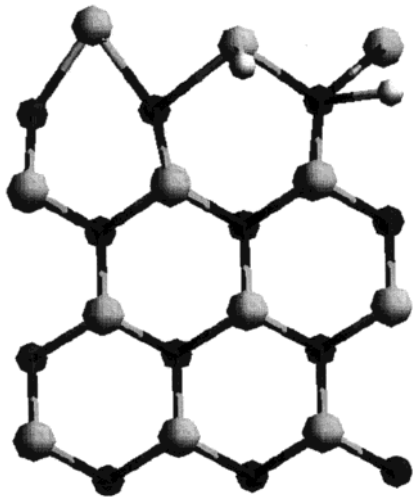

Figure 10. Cell showing the monohydrogenated MoS_2 sulfur edge; stable when -0.13 eV $< \alpha(T,P) < -0.01$ eV.

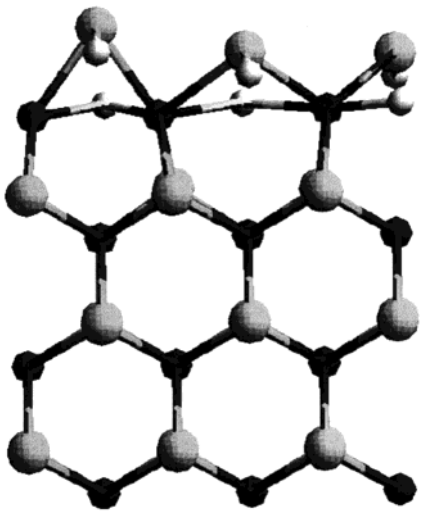

Figure 11. Cell showing the trihydrogenated MoS_2 sulfur edge; stable when $\alpha(T,P) < -0.13$ eV.

It can also be seen in the diagram in Figure 7 that H_2 dissociation to form two S−H groups is thermodynamically possible if $\alpha(T,P) < -0.4$. However, even for such values, heterolytic dissociation into S−H and Mo−H groups gives a more stable surface. On this diagram the trace corresponding to the hydrogenation of a more lacunar structure on which large molecules could adsorb is also reported. The line corresponding to the energy of this surface is always significantly above the most stable one. This means that lacunary structure [*X*−2] remains unstable even if we consider hydrogen adsorption.

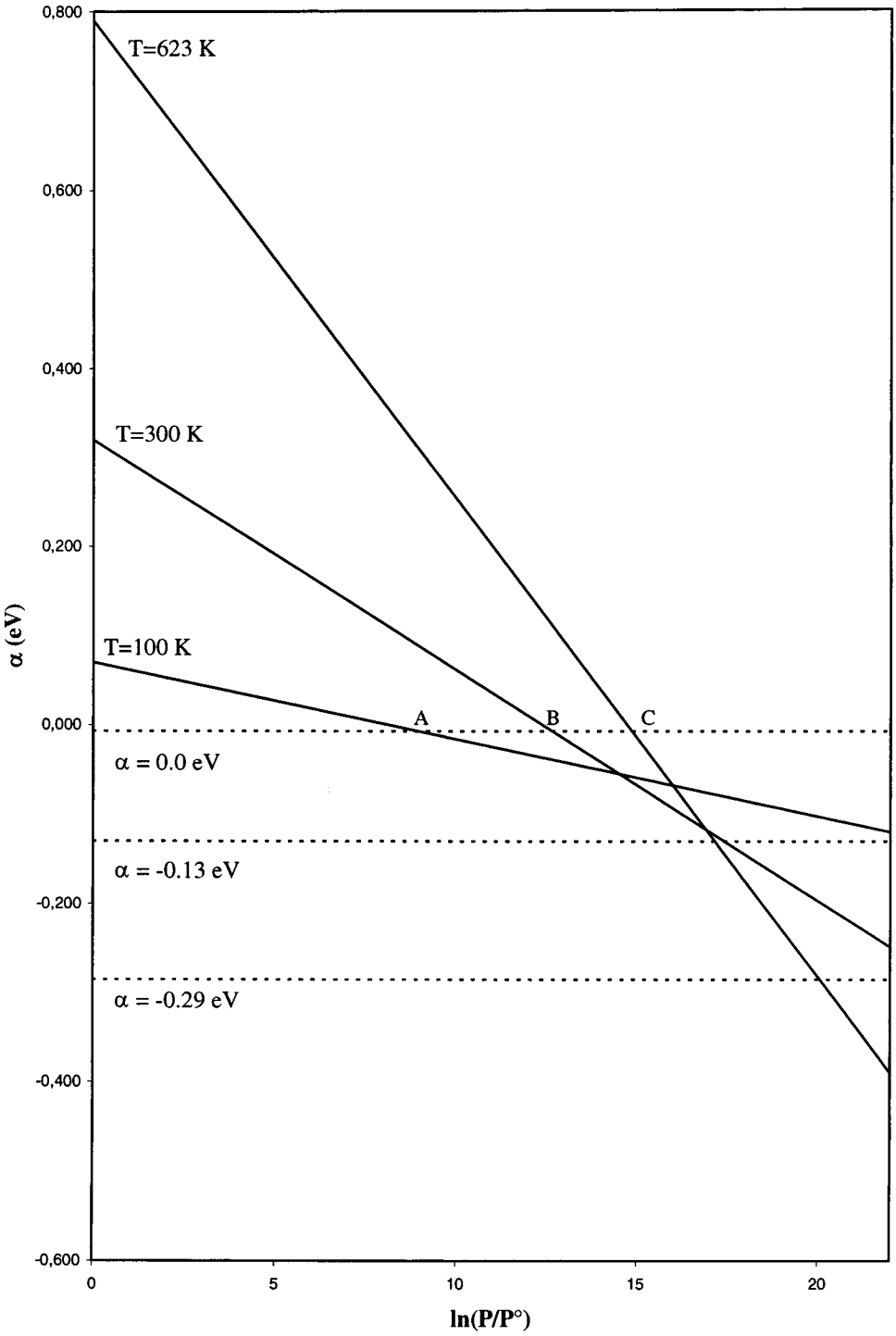

Figure 12. Evolution of $\alpha(T,P)$ as a function of $\ln(P/P°)$ for three different temperatures. The horizontal doted lines recalls the stability limits of the hydrogenated surfaces.

(b) Sulfur Edge [3−*X*]. The sulfur edge of the [3-*X*] surface behaves in the same way as the molybdenum edge upon H_2 addition and this behavior does not depend on the number of adsorbed hydrogen molecules. The most favored configuration is always the one producing the same amount of S−H groups and Mo−H groups. However, the first H_2 dissociation is almost athermic according to the electronic energy (see Table 5). This surface is therefore stable for low hydrogen chemical potential ($\alpha(T,P) \sim 0$ eV). The stability diagram versus the $\alpha(T,P)$ parameter is represented in Figure 9, in which three zones can be identified. In the first one, associated with high $\alpha(T,P)$ values, the stable surface does not have any hydrogen. The second zone corresponds to intermediate values of $\alpha(T,P)$ where the stable surface presents one S−H and one Mo−H group (cf. Figure 10). For $\alpha(T,P)$ lower than −0.19 eV, the surface is totally covered by hydrogen and presents three S−H and three Mo−H groups as shown in Figure 11.

From this diagram it can also be deduced that the creation of CUS on the sulfur edge is not possible even if hydrogen dissociation is taken into account as the corresponding hydrogenated lacunar [2−*X*] surface is less stable than surface [3−*X*] whatever the $\alpha(T,P)$ values.

4.3. Evaluation of $\alpha(T,P)$. In order to determine if hydrogen is present on the surface of the active phase in the hydrotreating

working conditions, we evaluate $\alpha(T,P)$

$$\alpha(T,P) = \Delta ZPE + RT \ln \frac{P(H_2)}{P^\circ}$$

As noted in section 4.2, H_2 dissociation will mainly produce one Mo−H and one S−H group. The vibrational modes of these groups will contribute to the energy, the main contribution originating from the stretching modes. The stretching mode, ν, of H_2 gas is observed at 4400 cm^{-1}. We estimate values of the stretching modes for Mo−H and S−H groups from literature data.[28] For S−H we have ν(S−H) at ca. 2500−2600 cm^{-1} and ν(Mo−H) at ca. 1750−1850 cm^{-1}. Assuming mean values, i.e., 2550 and 1800 cm^{-1} for the MoS−H and Mo−H stretching modes, respectively, we may estimate a mean Δ(ZPE) according to the following, equation that is ca. zero.

$$ZPE(H_{2surf}) - ZPE(H_2) = \frac{h\nu_1 + h\nu_2}{2} - \frac{h\nu(H_2)}{2} \approx 0$$

$RT \ln(q(H_2))$ was computed with H_2 partition functions for different temperatures and we drew the diagram represented in Figure 12, which gives the evolution of $\alpha(T,P)$ as a function of the total pressure for different temperatures. In this diagram are also reported the values of $\alpha(T,P)$ for which the various hydrogenated surfaces become stable. It shows that for $T =$ 623 K, $\alpha(T,P)$ remains positive until $\ln(P/P^\circ) = 14.8$ i.e., $P = 2.8 \times 10^{11}$ Pa (point C). According to the aforementioned domain of stability of the hydrogenated surface (section 4.2), it can be considered that hydrogen is not present on the edges of the crystallites at high temperature. Hydrogen on the MoS_2 surface could only be observed at low temperature and high pressure. At lower temperatures, a smaller pressure is needed to observe a quantitative H_2 adsorption on the surface. For example, for $T = 100$ K, $\alpha(T,P)$ becomes negative for $P = 7.7 \times 10^8$ Pa (point A) and for $T = 300$ K, $\alpha(T,P)$ becomes negative for $P = 6.5 \times 10^9$ Pa (point B). Under such conditions, one hydrogen molecule should be dissociated on the sulfur edge of the MoS_2 surface.

4.4. Comparison with Experiments. The free enthalpy cost for H_2 dissociation on the edge surfaces into Mo−H and S−H groups in the hydrotreating conditions ($T = 350$ °C; $P = 50$ bar; $\alpha(T,P) = 0.58$ eV) can be deduced from the aforementioned calculations. In such conditions, H_2 dissociation on the sulfur edge will require 0.55 eV and will produce one Mo−H and one S−H group. H_2 dissociation on the molybdenum edge will produce the same groups and require 0.85 eV. Even if this dissociation is easier on the sulfur edge than on the molybdenum one, this study shows that, under a reductive atmosphere, hydrogen is not stable on surface [3−3] of the active MoS_2 nanocrystallites. However, mechanistic studies require the presence of such hydrogen species that could therefore only be present at low coverage or as metastable species.

Direct evidence of S−H group on MoS_2 supported catalysts has never been reported to our knowledge. Assumption for the presence of such groups is always based on their indirect characterization. Indeed Mauge et al.[29] showed the presence of a Brönsted acidity through the adsorption of probe molecules, whereas Topsoe et al.[30] showed the creation of some new OH groups due to H_2S dissociative adsorption. Only Moyes et al.[31] reported an inelastic neutron spectroscopic (INS) study of MoS_2 pretreated under high H_2 pressure, in which they observed a line at 650 cm^{-1} that they assigned to a Mo−S−H deformation mode. But whatever the solid, bulk or supported, the presence of Mo−H groups has never been evidenced. We can assume that no hydrogen species are present on the edge surfaces as suggested by our calculations. We can therefore consider that in the Moyes' paper the hydrogen adsorption proceeded on the sulfur atoms of the basal plane as has been suggested by Muller[32] from IETS and Raman study.

5. Conclusion

This paper presents a DFT approach of molybdenum disulfide (100) edges where the HDS active sites are considered to be located. It has been shown that the sulfur coverage of both kinds of edges depends only on the H_2S/H_2 partial pressure ratio in the gas phase, and that the [3−3] surface is the most stable surface in high hydrogen chemical potential that should correspond to the working conditions of the catalyst. However, depending on the experimental conditions, the H_2S/H_2 ratio could increase (at the end of a catalytic test in a batch experiment or close to the bottom of the reactor in an industrial unit for example) and the stable surface could be surface [6−3] making the creation of vacancies on the sulfur edge more difficult. The investigation of H_2 dissociation on this surface is under progress. Whatever the conditions, the stable surface does not present any CUS allowing adsorption of large sulfur containing molecules. Such active site should thus be created by reaction with hydrogen. H_2 dissociation has been therefore considered on surface [3−3] that is the stable surface under high hydrogen chemical potential. It has been shown that the heterolytic dissociation into S−H and Mo−H groups is the least unstable. H_2 dissociation on a lacunar structure has also been considered showing that it can be athermic or slightly exothermic but this does not balance the sulfur removal energetic cost needed for the creation of the CUS. Lacunar structures remain thus unstable even if we consider hydrogen adsorption.

Acknowledgment. This work has been performed within the GdR Dynamique Moléculaire Quantique Appliquée à la Catalyse, a joint project of Centre National de la Recherche Scientifique (CNRS), Universität Wien (UW), Institut Français du pétrole (IFP), TOTALFINA, and Schuit Institute of Catalysis.

References and Notes

(1) Payen, E.; Hubaut, R.; Kasztelan, S.; Poulet, O.; Grimblot, J. *J. Catal* **1994**, *147*, 123.
(2) Prins, R.; De Beer, V. H. J.; Somorjai, G. A. *Catal. Rev. Sc. Eng.* **1989**, *31*, 1.
(3) Harris, S.; Chianelli, R. *J. Catal.* **1984**, *86*, 400.
(4) Mitchell, P. C. H.; Plant, C. *Bull. Soc. Chim. Belg.* **1995**, *104*, 293.
(5) Faye, P.; Payen E.; Bougeard, D. *J. Mol. Model.* **1999**, *5*, 63.
(6) Byskov, L. S.; Norskov, J. K.; Clausen, B. J.; Topsoe, H. *J. Catal.* **1999**, *187*, 109.
(7) Raybaud, P.; Hafner, J.; Kresse, G.; Toulhoat, H. *Surf. Sci.* **1998**, *407*, 237.
(8) Raybaud, P. Hafner, J.; Kresse, G.; Kasztelan, S.; Toulhoat, H. *J. Catal.* **2000**, *189*, 129.
(9) Kresse, G.; Hafner, J. *Phys. Rev. B* **1993**, 47, 558; **1994**, *49*, 14251. Kresse, G.; Furthmüller, J. *Comput. Mater. Sci*. **1996**, *6*, 15. Kresse, G.; Furthmüller, J. *Phys. Rev. B.* **1996**, *54*, 11169.
(10) Mermin, N. D. *Phys. Rev.* **1965**, *137*, A1141.
(11) Vanderbilt, D. *Phys. Rev. B.* **1980**, *41*, 7892. Kresse, G.; Hafner, J. *J. Phys.: Condens. Matter* **1994**, *6*, 8245.
(12) Methfessel, M.; Paxton, A. T. *Phys. Rev. B* **1989**, *40*, 3616.
(13) Perdew, J. P.; Zunger, A. *Phys. Rev. B.* **1981**, *23*, 5048.
(14) Perdew, J. P.; Chevary, J. A.; Vosko, S. H.; Jackson, K. A.; Pedersen, M. R.; Singh, D. J.; Frolais, C. *Phys. Rev. B* **1992**, *46*, 6671.
(15) Kadas, K.; Kern, G.; Hafner, J. *Phys. Rev. B* **1998**, *53*, 7649. Northrup, J. E. *Phys. Rev. B* **1991**, *44*, 1419. Scheffler, M. Presented at the European Congress on Catalysis, Rimini September 1999. Kaxiras, E.; Bar-Yam, Y.; Joannopoulos, J. D.; Pandey, K. C. *Phys. Rev. B* **1987**, *38*, 9625. Kaxiras, E.; Bar-Yam, Y.; Joannopoulos, J. D.; Pandey, K. C. *Phys. Rev. B* **1987**, *38*, 9636.
(16) Atkins, P. W. *Physical Chemistry*, 5th ed.; Oxford University Press: London, 1990.

(17) Payen, E.; Kasztelan, S.; Houssenbay, S.; Szymanski, R.; Grimblot, J. *J. Phys. Chem.* **1989**, *93*, 6501.

(18) Kasztelan, S.; Touloat, H.; Grimblot, J.; Bonnelle, J. P. *Appl. Catal.* **1984**, *13*, 127.

(19) Calais, C.; Matsubayashi, N.; Geantet, C.; Yoshimura, Y.; Shimada, H.; Nishijima, A.; Lacroix, M.; Breysse, M. *J. Catal.* **1997**, *170*, 29.

(20) Shido, T.; Prins, R. *J. Phys. Chem. B* **1998**, *102*, 8426.

(21) Plazenet, G.; Payen, E.; Cristol, S.; Paul, J. F.; Lynch, J. *Phys. Chem. Chem. Phys.*, in press.

(22) Da Silva, P. Ph.D. Thesis, Université Paris VI, 1998.

(23) Whitehurst, D. D.; Isoda, T.; Mochida, I. *Adv. Catal.***1998**, *42*, 345. Gates, B. C.; Topsoe, H. *Polyhedron* **1997**, *16*, 3213.

(24) Cristol, S.; Paul, J. F.; Payen, E.; Bougeard, D.; Hafner, J.; Hutschka, F. *Stud. Surf. Sci. Catal.* **1999**, *127*, 327.

(25) Toulhoat, H.; Raybaud, P.; Kasztelan, S.; Kresse, G.; Hafner, J. *Catal. Today* **1999**, *50*, 629.

(26) Raybaud, P. Hafner, J.; Kresse, G.; Kasztelan, S.; Toulhoat, H. *J. Catal.* **2000**, *190*, 128.

(27) Leglise, J.; van Gestel, J. N. M.; Finot, L.; Duchet, J. C.; Dubois, J. L. *Cata Today* **1998**, *45*, 347. Kasztelan, S. In *Advances in Hydrotreating Catalysts II*; ACS, Division of Petroleum Chemistry: Washington, DC, August 1994. Meille, V.; Schulz, E.; Lemaire, M.; Vrinat, M. *Appl. Catal.* **1999**, *187*, 179.

(28) Gland, J. L.; Kollin, E. B.; Zaera, F. *Langmuir* **1988**, *4*, 118. Burrow, T. E.; Lazarowych, N. J.; Morris, R. H.; Lane, J.; Richards, R. L. *Polyhedron* **1989**, *8*, 1989.

(29) Mauge, F.; Travert, A. *Stud. Surf. Sci. Catal.***1999**, *127*, 269.

(30) Topsoe, N. Y.; Topsoe, H. *J. Catal.* **1993**, *139*, 641.

(31) Sundberg, P.; Moyes, R. B.; Tomkinson, J. *J. Bull. Soc. Chim. Belg.* **1991**, *100*, 967.

(32) Diemann, E.; Weber, T.; Müller, A. *J. Catal.* **1994**, *148*, 288.